ELSEVIER

Chemical Engineering Journal 77 (2000) 111–118

Chemical Engineering Journal

www.elsevier.com/locate/cej

Chemical species tomography by near infra-red absorption

S.J. Carey [a], H. McCann [a,*], F.P. Hindle [a], K.B. Ozanyan [a], D.E. Winterbone [b], E. Clough [b]

[a] *Department of Electrical Engineering and Electronics, UMIST, Manchester M60 1QD, UK*

[b] *Department of Mechanical Engineering, UMIST, Manchester M60 1QD, UK*

Abstract

The spatial distribution of chemical species can be a critical determinant of the performance of chemical reactors. One such reactor is the combustion chamber of the Internal Combustion engine. This paper presents a design for the measurement of hydrocarbon concentration distribution within a running engine using near infra-red absorption tomography. The fundamentals of the technique, and design parameters for the equipment are discussed. By utilising micro-optic components, a minimally invasive system is feasible and by utilising advanced laser/photodetector combinations, good temporal performance is anticipated. ©2000 Elsevier Science S.A. All rights reserved.

Keywords: Tomography; Combustion; Infra-red; Spectroscopy

1. Introduction

In many chemical processes of industrial or commercial interest, the relevant reactions take place over extended regions of space with rates that are dependent on factors, such as mixture homogeneity or distribution, temperature and pressure. The study of systems containing liquid reactants has shown the benefits of electrical resistance tomography for measurement of species distribution [1].

In cases where there is little contrast due to bulk physical or electrical properties, there are presently very few techniques available to the researcher or process engineer that enable access to the distribution of chemical species.

The measurement of the distribution of gaseous species is of importance for applications, such as pollution monitoring and combustion research [2,3].

This paper presents an infra-red tomography technique that is applicable to the measurement of gaseous hydrocarbon distributions. The particular application targeted is the measurement of gasoline vapour distribution within the combustion chamber of an internal combustion engine.

1.1. Absorption spectroscopy and tomography

The transmission of light from a wavelength-swept narrow band source through an unknown chemical species can provide the means for its complete or partial identification, given that the species has a number of identifiable absorption bands within the wavelength range of the source.

When determining concentration of a species known to be present, a wavelength-swept source is generally not required; a single absorbed wavelength can be chosen, with absorption strength relating to concentration. However, other contributions to the received signal (ambient light, contaminant-induced absorption) must be accounted for.

Many gaseous species absorb light in the near infra-red region of the electromagnetic spectrum (1–2.5 μm). Table 1 gives peak absorptive wavelengths (within part of the near infra-red) for several species related to combustion research. These will be amenable to measurement with the general techniques and systems developed in this work.

However, absorption of a single transmitted beam through a gas cloud (Fig. 1) only tells us average concentration along a path. If the material is heterogeneous, a large number of different views through the object, followed by tomographic reconstruction, enables the concentration variation within the cloud to be determined. For non-parallel beams with irregularly placed detectors, algebraic reconstruction techniques (ART) are the most appropriate [4].

1.2. Imaging in the internal combustion engine

This paper is concerned with the design of a near infra-red tomographic system for the measurement of hydrocarbon concentration distribution within the cylinder of an internal combustion engine. The system will exploit the weak absorption of long chain hydrocarbons at 1.7 μm (see Table 1).

* Corresponding author. Tel.: +44-161-200-4703; fax: +44-161-200-4782.
E-mail address: h.mccann@umist.ac.uk (H. McCann).

PII: S1385-8947(99)00139-4

Table 1
Species absorbing light in the near infra-red

Species	Formula	Absorption wavelength in NIR(nm)
Nitric oxide	NO	1800
Carbon dioxide	CO_2	1960
Methane	CH_4	1650
Water	H_2O	1390
Carbon monoxide	CO	1570
Ethyne	C_2H_2	1520
Long chain HC's–partial saturation	–	1700

The measurement of hydrocarbon concentration within an internal combustion engine provides engine researchers with information on the efficacy of, for example, new combustion chamber designs and fuelling strategies [3,5]. However, the tools currently available (see Section 1.3) require considerable changes to the engine and combustion chamber, suffer from poor temporal performance and are costly. The design proposed here aims to produce an all opto-electronic system that allows flexible and reliable measurements at high image rates.

The target specification of the system is as follows:

1. Temporal resolution of 1 frame/°CA (crank angle) at 2000 rpm;
2. Spatial resolution of better than *D*/5, where *D*, the chamber diameter, is approximately 85 mm for a typical engine cylinder;
3. Hydrocarbon measurement precision of 5% of stoichiometry at 10 bar.

1.3. Techniques for engine applications

Planar Laser-Induced Fluorescence typically exploits detection of fluorescence at 90° to the direction of the stimulation beam [3,6–8]. Most implementations of this scheme involve the replacement of part of the cylinder wall with large glass windows through which the stimulant high energy pulsed laser beam is directed in a sheet form. A further window and mirror mounted on an extended piston directs fluorescence from the mixture onto a camera, typically a low-noise CCD array. The implementation of the system is necessarily complex in that the modifications to the engine are very severe. In general, a model single-component fuel is used, usually iso-octane, with fluorescent dopants added, 3-pentanone being most widely used. In addition, data can only be obtained at the repetition rate of the pulsed laser, limited to 100 Hz [8], and typically 1 Hz.

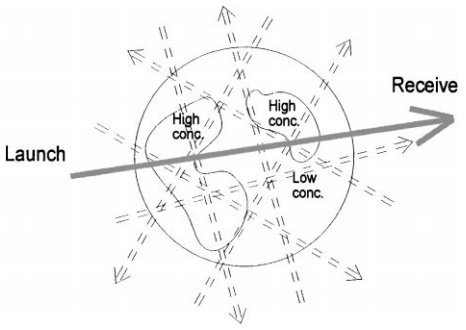

Fig. 1. Schematic diagram of transmission paths through a gas cloud of variable concentration, for tomographic reconstruction.

Previous attempts to monitor gaseous hydrocarbons by absorption [9–12] have also required large-scale optical access. Flame and soot emission studies [13–15] generally require the least degree of optical access. The measurements of flame emission clearly do not detect hydrocarbon presence directly; however, minimal optical access by inclusion of fibres and micro-optic lenses in the cylinder wall is appealing. The emission study of [15] additionally achieves soot monitoring, via monitoring of light at 650 nm. However, monitoring of hydrocarbon motion within a single cycle has not been realised. The repeatability of hydrocarbon combustion from cycle to cycle is of critical importance to engine researchers [16].

Clearly, in this application, use of one of the stronger absorption lines of iso-octane could be beneficial. However, although such a solution could be initially developed in the laboratory, a compact and portable implementation is desirable. Therefore, it is crucial to identify an all opto-electronic solution early in the design phase. As semiconductor technology advances, there is every reason to expect that the spectral range covered by laser diodes and photodetectors will be extended into the mid-IR by incorporating, amongst others, Sb-based technologies [17]. However, laser diodes are currently only commercially available up to a wavelength of around 2 μm.

Another important factor relating to species-specific detection is the need for wavelength tunability, or alternatively, precision manufacture of a laser to fulfil a wavelength requirement. With diode lasers, this can be achieved by a number of means, the largest tunability ranges being attained by use of extended cavity laser diodes. Smaller wavelength changes can also be generated by precise control of laser temperature and current. Hence, in cases when the peak absorption is strong, and therefore, the penetration depth is not sufficient for reliable imaging, the laser wavelength could, in principle, be tuned across the slopes of the absorption band to achieve the optimal values for absorptivity. For example,

availability of such tunable diode lasers at 3.4 μm may in the future open up a possibility to exploit the fundamental absorption band of long-chain hydrocarbons, instead of its second harmonic, as currently feasible and described here.

2. NIR tomography

In order to achieve good image quality, several competing effects to species-dependent absorption have to be overcome: scattering due to fuel droplets, contamination of optical components and blackbody radiation [11,12,15,18].

2.1. Theory

The transmitted light through a distance x, of a uniformly absorbing material is given by the Beer–Lambert law:

$$I_r(\lambda) = I_o(\lambda)\, e^{-\alpha(\lambda)cx} \quad (1)$$

where: $I_r(\lambda)$=received light intensity at wavelength λ; $I_o(\lambda)$=launched light intensity at λ; $\alpha(\lambda)$=absorptivity at λ; c=molar concentration.

In the case considered, where the receiver is operating in an environment of high temperature, blackbody radiation adds to the received signal. In addition, other effects (e.g. scattering) must be accounted for by modifying Eq. (1) as follows:

$$I_r(\lambda) = I_o(\lambda)\, e^{-\alpha(\lambda)cx} F + I_T \quad (2)$$

where F is the attenuation due to mechanisms which are not specific to the hydrocarbon species of interest, as discussed above. I_T is the intensity due to thermal background radiation.

When the gas concentration is not uniform, the received light intensity after transmission across a path L is given by:

$$I_r(\lambda) = I_o(\lambda)\exp\left(-\int_L \alpha(\lambda)c(x, y)\, dl\right) F_L + I_{TL} \quad (3)$$

where F_L is specific to each particular path (over the time of the measurement) and I_{TL} is specific to the viewing path of the receiving optics (at the measurement time).

The necessary information for tomographic reconstruction from several path-integrated measurements is contained within the exponent in Eq. (3). Therefore, the measurement strategy must be designed to determine the above integral.

Using two different wavelengths, λ_1 and λ_2, effects common to both wavelengths (i.e. F_L) can be removed, leaving a path-concentration integral given by:

$$\int_L c(x, y)\, dl = \frac{1}{\alpha(\lambda_1) - \alpha(\lambda_2)} \ln\left(\frac{I_r(\lambda_2) - I_{TL}}{I_r(\lambda_1) - I_{TL}} \frac{I_o(\lambda_1)}{I_o(\lambda_2)}\right) \quad (4)$$

In general, λ_1 and λ_2 are chosen such that the chemically specific absorptivity at wavelength λ_1 (i.e. $\alpha(\lambda_1)$), is large due to resonant vibrational/rotational transitions, and the absorption at λ_2 is dominated by non-resonant, non-chemically specific attenuation mechanisms, that is, $\alpha(\lambda_2)$ is small, although F_L may be significant. λ_2 is termed the 'reference' wavelength.

Hence, the data we require from each beam path are the launch powers at each wavelength (which should be constant over a long period), updated values of received power at each wavelength and a value for blackbody radiation. The received light values at each wavelength should be collected simultaneously for all beam paths.

2.2. System considerations and technologies

Within the near infra-red wavelength region, there are a number of available technologies as described in the following sections.

2.2.1. Fibres

Silica fibre is useably transmissive for fibre optic sensors between 300 and 2100 nm (attenuation staying below $\sim$0.1 dBm^{-1}). Hence this is the fibre of choice.

2.2.2. Detectors

Available detectors in the near infra-red are shown in Table 2. Detectivity is given at 1.7 μm for relevance to this work.

For the purposes of this work, IGA and extended IGA devices appear to offer the best performance prospects.

2.2.3. Multiplexing/de-multiplexing

The transmission at each of the two wavelengths for each beam path must be determined at the receivers. This can be

Table 2
Detector options for near infra-red

Detector technology	D* at 1.7 μm at 20°C (cm W^{-1} $Hz^{1/2}$]	Operating wavelength (nm)
Ge	3.0×10^{10}	700–1800
InGaAs (IGA)	8.0×10^{11}[a]	800–1700
Extended IGA InGaAsSb/InAsSbP	2.0×10^{11}	1000–2100 or 2600
InAs	5×10^{8}	1000–3800
PbS	4×10^{10}	1000–3300
PbSe	5×10^{9}	1000–4500
InSb	2×10^{10} (77 K)	1000–5500

[a] Assumes 0.15A/W responsivity.

made possible by optical wavelength de-multiplexing onto separate photodiodes, or, by wavelength encoding by means of time division or frequency multiplexing. Techniques for the former (optical de-multiplexing), and attributes, are as follows:

1. Multi-layer filters — expensive since lens/filter assemblies are also required;
2. Fibre-optic fused biconical taper couplers — expensive; poor isolation and high insertion loss if wavelengths close;
3. Multi-mode fibre WDM — lossy;
4. Integrated optic fibre components — expensive;
5. Spatial filtering — requires two launch systems; expensive; potential deleterious effects on reconstructed image.

Of these techniques, a bespoke multi-mode WDM may be the most cost-effective solution. However, all solutions would require a second array of detectors and would result in a lack of flexibility and upgradeability in laser wavelength. Hence electronic multiplexing in frequency or time domains is favoured.

2.2.4. Lasers/LEDs

Since we have a requirement to modulate the sources, there are a number of options:

1. Diode lasers — using amplitude modulation, via the drive current;
2. OPO based laser systems — with an appropriate pulse repetition frequency;
3. Gas lasers — with an external amplitude modulator.

At present, the spectral shapes of LED sources are too broad for this application, although work underway with resonant cavity-enhanced LEDs is promising [19]. Ideally, the spectral characteristics of IR sources should be selected with respect to linewidth as well as central wavelength; too narrow a linewidth can lead to system instabilities related to etalon/speckle effects [10] and species temperature/pressure change through spectral broadening.

A customised 1700 nm laser has been manufactured for this project.

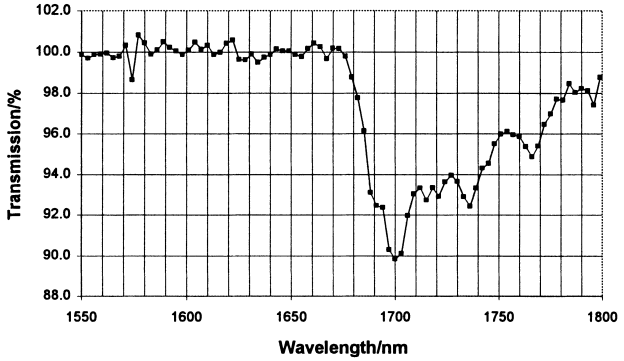

Fig. 2. Pressurised chamber for gaseous spectral absorption analysis.

3. Infra-red absorption in a combustion environment

The primary fuel considered in this study is iso-octane (2,2,4 tri-methylpentane). The absorption lines utilised in previous studies were 3.4 [9,11] and 2.3 μm [12]. This study proposes the use of the second harmonic of the C–H stretch mode at 1.7 μm. Spectra are generally available for liquid phase species [20,21]; less so for the gaseous phase. Using a single channel pressurised chamber built at UMIST (Fig. 2), the spectral absorbance of gaseous iso-octane in the wavelength region of interest was determined (however, independent calibration of vapour concentration has not been

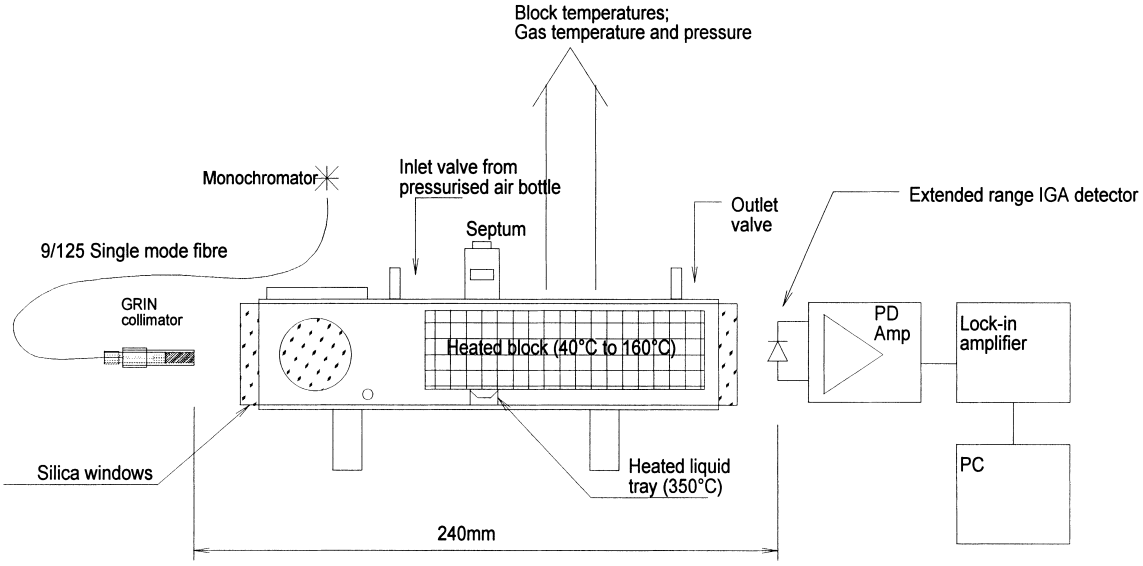

Fig. 3. Transmission of gaseous iso-octane: 10 bar, 80°C, 0.0073 mol l^{-1}; 164 mm path length; 5 nm source bandwidth; normalised to 100% transmission at 1650 nm.

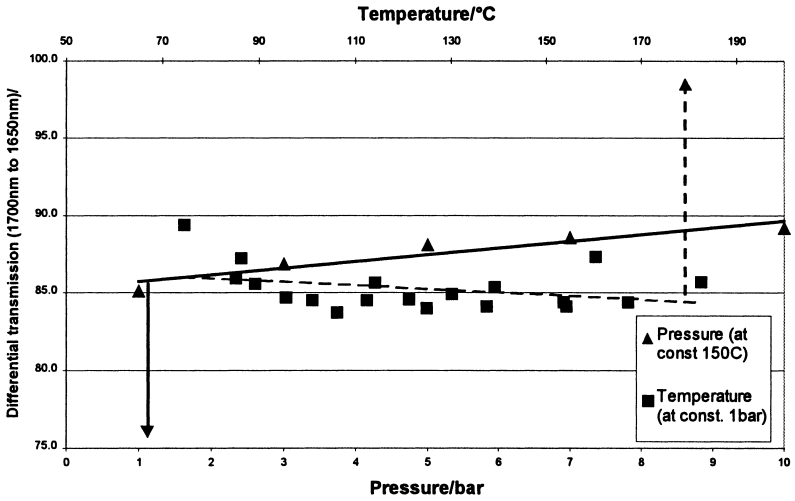

Fig. 4. Peak absorption of gaseous iso-octane at 1700 nm with changing temperature (at pressure of 1 bar) and changing pressure (at temperature of 150°C); 5 nm source bandwidth; 164 mm path length; 0.0073 mol l^{-1} concentration.

completed at the time of writing). This yields the absorption spectrum for a typical path in an internal combustion engine as shown in Fig. 3. The peak absorption wavelength occurs at 1700 nm. Whilst the linewidth of this peak is dominated by absorption effects, the linewidth of the source prevented determination of any potential fine structure in the spectroscopy of the gas. This remains a matter for further study.

Studies of the variation of iso-octane absorption with temperature and pressure are underway. Some preliminary sample data are shown in Fig. 4.

The requirement for the reference wavelength is that it should be largely unabsorbed by both the measured species and other species that may be present in the combustion chamber, that is primarily water and carbon dioxide. Utilising the USAF's MODTRAN 3.7 software and database (part of the HAWKS compilation [22]) provides an insight into the likely absorption resulting from these species as shown in Figs. 5 and 6. From this data, it appears that a wavelength between 1500 and 1670 nm would be suitable as a reference.

4. Instrument architecture

4.1. Optical system design

The proposed system architecture is shown in Fig. 7. The system design (to the point of light reception) attempts to utilise many components primarily designed for telecommunications (couplers, fibres, photodiodes).

The aim of the opto-electronic design is to achieve adequate signal to noise in terms of the integrated concentration along a path. For use in ART image reconstruction, the noise characteristics of the signals must in turn meet the precision requirement for the reconstructed image (see Section 1.2).

For the purposes of illustration, we assume here that the thermal background is negligible, and errors in determining the path integral are dominated by the noise in the received photocurrent. Through error analysis, the signal to noise ratio in the calculated path-concentration integral, N_{PCI}, is given by the following approximate expression for small values of absorption:

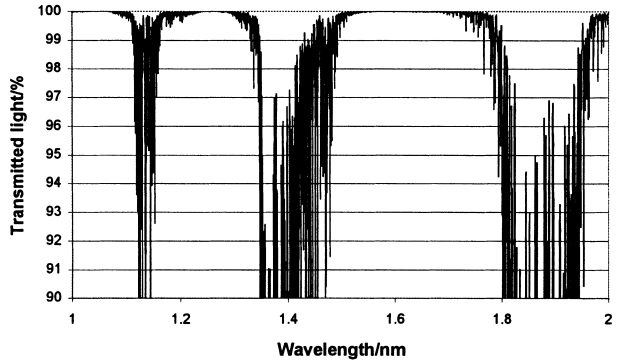

Fig. 5. Light transmission for water vapour: concentration 134,000 ppm; 85 mm path length; 1 cm^{-1} source resolution; 10 bar, 500°C.

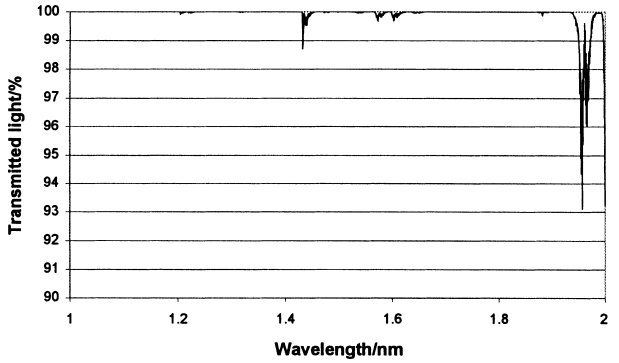

Fig. 6. Light transmission for carbon dioxide: concentration 119,000 ppm; 85 mm path length; 1 cm^{-1} source resolution; 10 bar; 500°C.

$$N_{\mathrm{PCI}} = \frac{i_{\mathrm{s}} A_{\lambda}}{\sqrt{2} i_{\mathrm{n}}} \tag{5}$$

where A_{λ}=fractional absorption at λ ($i_{\mathrm{s}}A_{\lambda}$ represents the useful signal within a single measurement); i_{s}=average photocurrent (photocurrents due to the two lasers are assumed equal); i_{n}=noise current.

Now

$$\frac{i_{\mathrm{s}}}{i_{\mathrm{n}}} N_{\mathrm{fe}} \tag{6}$$

where N_{fe} is the signal to noise requirement of the signal emerging from the front end amplifier. For A_{λ}=0.04 (for a representative stoichiometric mix of iso-octane across a 85 mm path length) and N_{PCI}=20 (i.e. the signal to noise requirement of the path concentration integral has been set at the same as that of the pixel precision requirement of 5%), the front end signal to noise requirement, N_{fe} is 700.

To determine the noise current (i_{n}) explicitly, we must add the contributions from the following noise sources:

1. Amplifier current and voltage noise
2. Shot noise
3. Johnson noise from resistances in the photodiode and amplifier system

In calculating the noise generated by the generic photodiode amplifier, the gain with respect to frequency of the above noise sources must be determined. Then the total noise can be found by integrating the noise over the frequency band of interest. In relation to this work, however, the shot noise and amplifier voltage noise will dominate.

A computer analysis has been made for the photodiode (based on an extended InGaAs photodiode; see Section 4.2) and amplifier system proposed here. This analysis shows that using a lock-in amplifier (which restricts bandwidth), a peak power of 1 μW at each photodiode should provide a signal to noise ratio of approximately 5000. However, additional noise will also arise from the effects of de-multiplexing and the reconstruction process. These will be determined as system build progresses.

In determining the total laser power required, an account must be made of the optical loss between the lasers and light reception at the photodiodes (see Fig. 7) as shown in Table 3.

The table shows that around 1000 times more power is required at the laser as is at the photodiode. Typical laser diode outputs are in the region of 1–5 mW. Hence it is expected that a single laser diode operating at each wavelength should be sufficient for successful system operation.

Table 3
Optical power budget for 96 channel system

Coupling to detector	−1.5 dB
Link loss (via cylinder)	−3.5 dB
1×32 coupler	−19 dB
Broadband couplers	−6 dB
WDM loss	−1 dB
Total insertion loss	−31.0 dB

4.2. Photodetectors

Requirements of the photodetector for this application are to:

1. Show good responsivity at 1700 nm.
2. Couple with high efficiency from large core receiving fibres.
3. Have low capacitance (and hence low noise and high bandwidth).
4. Have low cost (due to their significant number).

The responsivity issue is of particular concern since IGA photodiodes (developed mainly for telecommunication applications) cease to be responsive around 1700 nm. A number of devices were characterised as shown in Fig. 8.

Suitable photodiodes are extended IGA devices or, at the margin, selected standard IGA devices. The latter have the advantages of:

- lower capacitance (and hence higher bandwidth and lower noise);
- higher shunt resistance (and hence lower noise);
- low cost;

and the following disadvantages:

- high temperature sensitivity at 1700 nm;
- lack of response above 1700 nm to allow for system upgrades and changes.

Hence the final choice of photodiode is finely balanced; to allow for prototype development, extended IGA diodes are preferred.

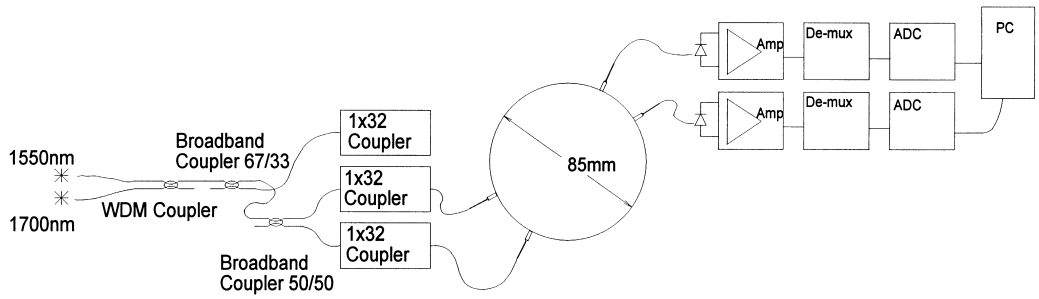

Fig. 7. Proposed optical tomography system design.

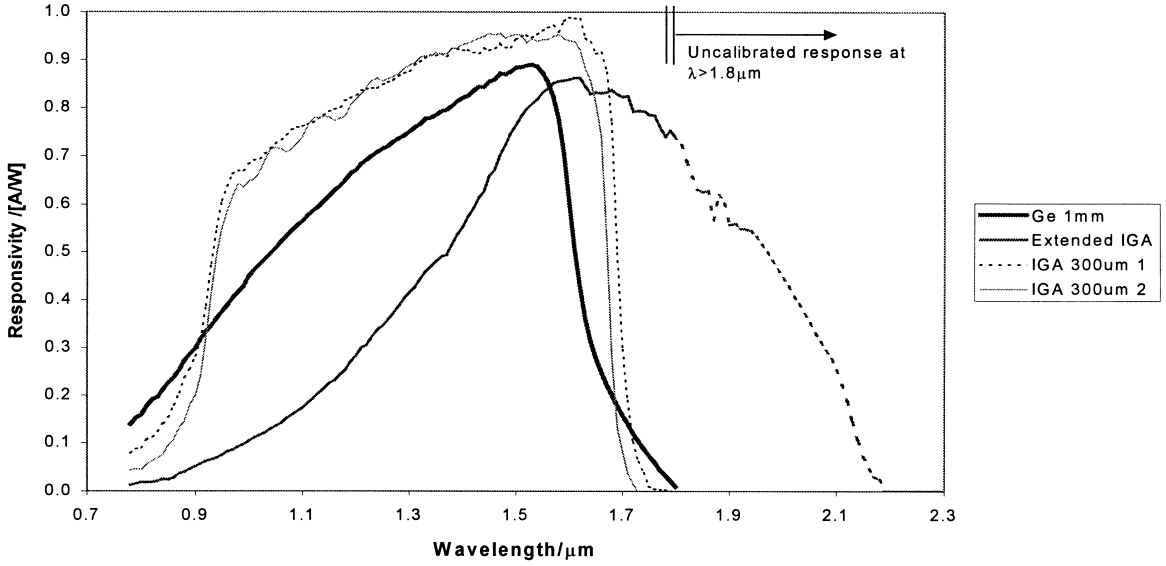

Fig. 8. Responsivity of photodiodes.

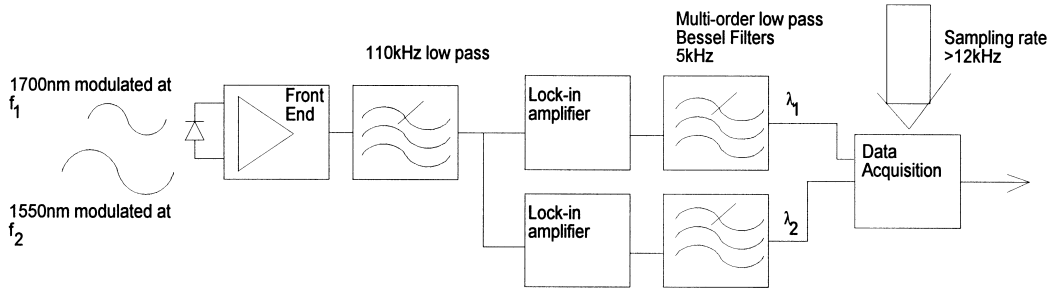

Fig. 9. De-multiplexing scheme.

4.3. Multiplexing system

There are a number of options for signal coding including frequency division multiplexing (FDM), time division multiplexing (TDM) and optical filtering of signals (see Section 2.2). Of these, the most appealing is FDM (Fig. 9), since it enables lock-in detection to be utilised at the receiver. This in turn enables the lowest noise coupling and incorporation of anti-aliasing filters (which would be more difficult to incorporate in a TDM system). A system design for TDM also requires the incorporation of a method of measuring thermal background radiation. For FDM, thermal background is automatically removed if modulation frequencies are chosen carefully; however, thermal emission is a useful measurand in itself if flame emission information is required.

4.4. Opto-mechanics

The manner in which the optical components can be assembled to allow access to a combustion chamber is critical to the system's success. Fig. 10 shows a system incorporating 28 channels. Work is underway to increase this number.

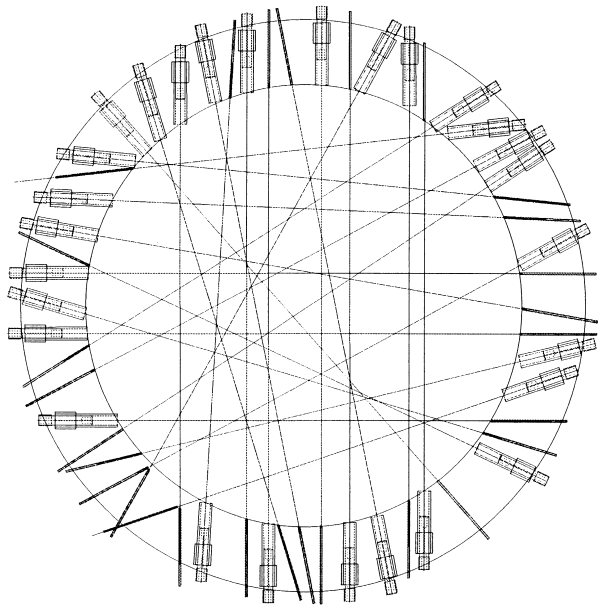

Fig. 10. 28 channel system.

A particular challenge in this regard is the physical space available for the total of 190 launch and receive fibres which appear to be feasible from power budget calculations. Use of fan beam optics [10] will reduce this number but at the expense of higher insertion loss.

5. Conclusions

A near infra-red tomography system has been designed for the specific application of mapping hydrocarbon concentration in a combustion environment. An effective system appears to be feasible in spite of weak absorption at the selected wavelength of 1.7 μm. Problems still exist due to space constraints around an 85 mm diameter cylinder.

The expanding use of laser diodes, photodetectors and associated components (especially in telecommunications) will enable a cost-effective all opto-electronic solution to be implemented. The general engineering and spectroscopic principles exploited here are believed to be applicable to other chemical system measurement applications.

Acknowledgements

SJC, HMcC, FPH and KBO are members of the Virtual Centre for Industrial Process Tomography. The support of EPSRC is acknowledged via GR/L67592. The authors are grateful for helpful discussions with Stan Wallace (Rover Group), Steve Nattrass (Shell Research).

References

[1] P.J. Holden, M. Wang, R. Mann, F.J. Dickin, R.B. Edwards, Imaging stirred-vessel macromixing using electrical resistance tomography, AIChE J. 44 (4) (1998) 780–790.
[2] R. Grisar, et al. (Eds.), Monitoring of Gaseous Pollutants by Tunable Diode Lasers, Proceedings of Third International Symposium, October 1991, Kluwer, Dordrecht, 1992.
[3] M. Berckmuller, N.P. Tait, D.A. Greenhalgh, The time history of the mixture formation process in a lean burn stratified-charge engine, SAE 961929.
[4] R.G. Jackson, The development of optical systems for process imaging, in: R.A. Williams, M.S. Beck (Eds.), Process Tomography – Principles, Techniques and Applications, Butterworth-Heinemann, London, 1995.
[5] Direct Injection SI Engine Technology, SAE SP-1314, Warrendale, USA, 1998.
[6] D.A. Greenhalgh, in: L. Lading, S. Wigley, P. Buchhave (Eds.), Optical Diagnostics for Flow Processes, Plenum Press, New York, 1994 and references therein.
[7] F. Hildenbrand, C. Schultz, V. Sick, G. Josefsson, I. Magnusson, O. Andersson, M. Alden, Laser spectroscopic investigation of flow fields and NO- formation in a realistic SI engine, Vol. 1348, SAE Special Publications, February 1998, pp. 107–116 (Analysis of Combustion and Flow Diagnostics)
[8] E. Winklhofer, H. Fuchs, Laser induced fluorescence and flame photography – tools in gasoline engine combustion analysis, Optics Lasers Eng. 25 (6) (1996) 379–400.
[9] H. Kawazoe, K. Inagagi, Y. Emi, F. Yoshino, Computer tomography measurement of gaseous fuel concentration by infra-red laser light absorption, SPIE 3172 (1997) 576–584.
[10] E.J. Beiting, Fibre-optic fan-beam absorption tomography, Appl. Optics 31 (1992) 1328.
[11] E. Winklhofer, G.K. Fraidl, A. Plimon, Monitoring of gasoline fuel distribution in a research engine , Proc. I. Mech. E. 206 (1992) 107.
[12] S.M. Skippon, S.R. Nattrass, J.S. Kitching, L. Hardiman, H. Millar, Effects of fuel composition on in-cylinder air/fuel ratio during fuelling transients in an SI engine, measured using differential infra-red absorption, SAE 961204.
[13] U. Spicher et al., Application of a new optical fibre technique for flame propagation diagnostics in IC engines, SAE 881637.
[14] H. Philipp, A. Plimon, G. Fernitz, A. Hirsch, G. Fraidl, E. Winklhofer, A tomographic camera system for combustion diagnostics in SI engines, SAE 950681.
[15] A.E.M. Barrag, B. Lawton, Computer optical tomography in the study of internal combustion engine soot concentration, Proceedings of 26th International Symposium on Automotive Technology and Automation, Vol.: The motor vehicle and the environment – demands of the nineties and beyond, September 1993, Aachen.
[16] J.B. Heywood, Internal Combustion Engine Fundamentals, McGraw-Hill, New York, 1988.
[17] D.C. McCarthy, Photonics Spectra, February 1999, p. 38.
[18] S.R. Nattrass, D.M. Thompson, H. McCann, First in-situ measurement of lubrication degradation in the ring pack of a running engine, SAE 942026.
[19] B.M. Poole, K.E. Singer, M. Missous, Wafer bonded resonant-cavity light-emitting diodes for 1.7 μm emission, Conference Proceedings of Postgraduate Research in Electronics, Photonics and Related Fields, 5–7 January 1999, Manchester, Leeds University Press, 1999.
[20] M. Buback, H.P. Vogele, FT-NIR Atlas, VCH, Germany.
[21] The Atlas of Near Infra-Red Spectra, Sadtler/Heyden, Philadelphia/London, 1981.
[22] L.S. Rothman, C.P. Rinsland, A. Goldman, S.T. Massie, D.P. Edwards, J.-M. Flaud, A. Perrin, C. Camy-Peyrey, V. Dana, J.-Y. Mandin, J. Schroeder, A. McCann, R.R. Gamache, R.B. Wattsin, K. Yoshino, K.V. Chance, K.W. Juck, L.R. Brown, V. Nemtchechin, P. Varanasi, The HITRAN molecular spectroscopic database and HAWKS (HITRAN atmospheric workstation) 1996 edition, J. Quantitative Spectrosc. Radiative Trans. 60 (5) (1998) 665–710.